Published in final edited form as:
Mol Microbiol. 2007 June ; 64(6): 1515–1528. doi:10.1111/j.1365-2958.2007.05748.x.

Identification and characterization of the immunity repressor (ImmR) that controls the mobile genetic element ICE*Bs1* of *Bacillus subtilis*

Jennifer M. Auchtung, **Catherine A. Lee**, **Katherine L. Garrison**, and **Alan D. Grossman***
Department of Biology, Massachusetts Institute of Technology, Cambridge, MA 02139, USA

Summary

ICE*Bs1* is a mobile genetic element found in the chromosome of *Bacillus subtilis*. Excision and transfer of ICE*Bs1* is regulated by the global DNA damage response and intercellular peptide signalling. We identified and characterized a repressor, ImmR (formerly YdcN), encoded by ICE*Bs1*. ImmR represses transcription of genes required for excision and transfer, and both activates and represses its own transcription. ImmR regulates transcription within ICE*Bs1* by binding to several sites in the region of DNA that contains promoters for both *immR* and *xis* (encoding excisionase). In addition, we found that ImmR confers immunity from acquisition of additional copies of ICE*Bs1*. ImmR-mediated regulation serves to keep a single copy of ICE*Bs1* stably maintained in the absence of induction, allows a rapid response to inducing signals, and helps limit acquisition of additional copies of ICE*Bs1*.

Introduction

Mobile genetic elements play an important role in horizontal gene transfer and the evolution of bacterial species (reviewed in Ochman *et al*., 2000; Brussow *et al*., 2004; Burrus and Waldor, 2004; Frost *et al*., 2005). ICE*Bs1* is an integrative and conjugative element (also known as a conjugative transposon) found in the *Bacillus subtilis* chromosome (Burrus *et al*., 2002; Auchtung *et al*., 2005). ICE*Bs1* is normally propagated passively by the host cell through chromosomal replication and cell division. When the host cell undergoes DNA damage or ICE*Bs1*-containing cells are surrounded by cells lacking ICE*Bs1*, ICE*Bs1* can excise from the chromosome and transfer to recipient cells (Auchtung *et al*., 2005). Excision requires the site-specific recombinase, Int, and an accessory protein, Xis (C.A. Lee, J.M. Auchtung, R.E. Monson and A.D. Grossman, in preparation). Transfer requires several ICE*Bs1*-encoded conjugation proteins (C.A. Lee, M.B. Berkmen, and A.D. Grossman, unpublished results).

Most of the genes in ICE*Bs1* are located downstream from *xis* (Fig. 1) and transcription of most of these genes (*xis* through *yddJ*) appears to be co-regulated (Auchtung *et al*., 2005). The global DNA damage response stimulates expression of these genes, and leads to excision and mating of ICE*Bs1* (Auchtung *et al*., 2005). Thus, ICE*Bs1* has a mechanism to sense host cell genomic stress and initiate its escape from distressed cells.

Intercellular peptide signalling also regulates transcription of *xis* through *yddJ*, and excision and transfer of ICE*Bs1* (Auchtung *et al*., 2005). This regulation occurs independently of the global DNA damage response and is mediated by the *rapI-phrI* signalling cassette encoded

*For correspondence. adg@mit.edu; Tel. (+1) 617 253 1515; Fax (+1) 617 253 2643.

in ICE*Bs1*. RapI stimulates expression of *xis* through *yddJ* and this stimulatory activity is antagonized by the secreted signalling peptide, PhrI. PhrI is a pentapeptide that is re-imported through the oligopeptide permease (Auchtung *et al*., 2005). As *rapI* and *phrI* are contained in ICE*Bs1*, they function in self-recognition, inhibiting excision and transfer of ICE*Bs1* when other cells containing ICE*Bs1* are present. It is currently unknown how the global DNA damage response and RapI regulate transcription of *xis* through *yddJ*.

ICE*Bs1* encodes a putative repressor, ImmR, which was recognized based on homology to some bacteriophage repressors (Burrus *et al*., 2002; Auchtung *et al*., 2005). We investigated the role of *immR* (formerly *ydcN*) in regulating the activity of ICE*Bs1*. We found that ImmR represses transcription of the promoter that drives expression of *xis*. This repression is critical for preventing excision of ICE*Bs1* and expression of most of its genes (*xis* through *yddJ*). In addition, we found that ImmR activates and represses its own transcription and transcription of the two genes downstream, *ydcM* and *int*. Autoregulation likely allows the levels of ImmR to be maintained at concentrations high enough to repress transcription of *xis-yddJ* and low enough to respond efficiently to inducing signals. Furthermore, we found that ImmR functions as an immunity repressor. That is, when expressed in a potential recipient, it greatly reduces the frequency of acquisition of ICE*Bs1* via conjugation. This serves to limit acquisition of additional copies of ICE*Bs1* by cells already containing the element. Immunity conferred by ImmR can be suppressed by increased expression of *int*, indicating that ImmR mediates immunity by limiting expression or activity of integrase. Thus, ImmR functions to ensure stable maintenance of a single copy of ICE*Bs1* and to limit acquisition of additional copies.

Results

Characterization of the *xis* promoter

xis encodes a protein required for excision of ICE*Bs1* (C.A. Lee, J.M. Auchtung and A.D. Grossman, unpubl. results). It is the first gene in a putative operon (*xis* through *yddJ*) involved in excision and transfer of ICE*Bs1* (Fig. 1). Expression of these genes (*xis-yddJ*) increases dramatically in response to inducing conditions, such as overproduction of RapI or treatment of the cells with the DNA-damaging agent mitomycin C (MMC) (Auchtung *et al*., 2005).

We mapped the 5′ end of the *xis* transcript using primer extension analysis (Fig. 2A and B). In cells overexpressing *rapI* or treated with MMC, we detected an abundant RNA species with a 5′ end 39 nucleotides upstream of the *xis* start codon (Fig. 2B). Similar results were obtained using a different primer in the extension reactions (data not shown). We did not detect any primer extension product specific to *xis* using RNA from uninduced cells as template. These results indicate that there is a strong transcription start site upstream of *xis* that is induced by overproduction of RapI or treatment with MMC.

Just upstream of the position of the 5′ end of the *xis* mRNA there are potential −10 and −35 recognition elements for *B. subtilis* RNA polymerase containing the major sigma factor, sigma-A. The −10 sequence, TATAAT, is a perfect match to the consensus (Helmann, 1995). The −35 sequence, TTGACT, differs from the consensus in only one position (underlined). Together, the primer extension and DNA sequence indicate that transcription of *xis* likely initiates from a sigma-A-dependent promoter located upstream of *xis* and that transcription from this promoter increases dramatically under conditions known to induce ICE*Bs1* gene expression and excision.

To further study the *xis* promoter (P*xis*), we constructed a transcriptional fusion of the region upstream of *xis* (from −343 to −6 bp upstream of *xis* start codon; Fig. 2A) to *lacZ* and

integrated this fusion at an ectopic site in the chromosome. We found that P*xis–lacZ*Ω343 was expressed at very low levels in wild-type cells (Figs 2 and 3) and that expression increased substantially in response to overexpression of *rapI* (Fig. 2C) or treatment of cells with MMC (Fig. 2D). These results are in accordance with the results of transcriptional profiling (Auchtung *et al*., 2005) and primer extension analysis (Fig. 2B), and indicate that the region of DNA contained in the fusion contains the sequences necessary for appropriate regulation of transcription of *xis*.

Characterization of ImmR

ImmR (YdcN) is similar to some bacteriophage repressors (Burrus *et al*., 2002; Auchtung *et al*., 2005). We found that ImmR represses transcription from the *xis* promoter. Expression of P*xis–lacZ*Ω343 was low in cells containing ICE*Bs1* (Fig. 3A and B). In contrast, expression increased >1000-fold in ICE*Bs1*^{0} cells, that is, in cells cured of ICE*Bs1* (Fig. 3A). Expression of P*xis–lacZ*Ω343 in the ICE*Bs1*^{0} strain was repressed upon ectopic expression of *immR* (Fig. 3A). This repression was observed when *immR* was expressed ectopically from either the isopropyl-β-D-thiogalactopyranoside (IPTG)-inducible promoter, P*spank*, or its native promoter, P*immR* (Fig. 3A; see below). With P*spank-immR*, the amount of repression of P*xis–lacZ*Ω343 was dependent on the concentration of IPTG (Fig. 3A). Strong repression was observed at a high concentration of inducer (1 mM) and partial repression was observed at a lower concentration of inducer (0.025 mM). These results demonstrate that ImmR is the only ICE*Bs1*-encoded protein required for repression of the *xis* promoter and that ImmR represses *xis* transcription in a dose-dependent manner.

We also analysed the phenotype caused by an *immR* null mutation (Auchtung *et al*., 2005). This mutation caused an ~1000-fold increase in β-galactosidase-specific activity from P*xis–lacZ*Ω343 (Fig. 3B). This expression was reduced to near wild-type levels in the presence of P*spank-immR* (Fig. 3B). These complementation results indicate that the derepression of P*xis–lacZ*Ω343 observed in the *immR* null mutant was due to loss of *immR* and not a secondary or polar effect. In combination, these results indicate that ImmR is both necessary and sufficient to repress transcription from the *xis* promoter.

In addition to affecting expression of P*xis–lacZ*Ω343, deletion of *immR* caused excision of ICE*Bs1* in most cells (Fig. 3C and D). Increased excision in the *immR* mutant is likely due to increased expression of *xis*, because increased expression of *xis* alone is sufficient to stimulate ICE*Bs1* excision (C.A. Lee, J.M. Auchtung, R. Monson and A.D. Grossman, in preparation). The increase in excision in the *immR* mutant was suppressed by expression of P*spank-immR*, indicating that the increased excision was due to loss of *immR* (Fig. 3D). Furthermore, because of increased excision, ICE*Bs1* is unstable in the *immR* null mutant and is lost at a relatively high frequency; approximately 10% of cells in a population of the *immR* null mutant have lost ICE*Bs1* (Auchtung *et al*., 2005). We suspect that ICE*Bs1* is not lost from all cells due to replication of the excised element. The increase in P*xis–lacZ*Ω343 expression observed for the Δ*immR* mutant reflects the expression in the ~90% of cells in the population that are Δ*immR* and contain the element as well as the ~10% of cells that have lost ICE*Bs1*. Together, these data indicate that ImmR represses expression from the *xis* promoter, thereby repressing excision of ICE*Bs1*.

In the course of constructing and growing the *immR* null mutant, we noticed that there was increased lysis of mutant colonies during prolonged growth on agar plates (data not shown). Cells that were missing *immR* due to complete loss of ICE*Bs1* did not have increased lysis, indicating that the increased lysis was due to loss of *immR* combined with the presence of ICE*Bs1* and not due to some additional function of *immR* outside of the context of ICE*Bs1*.

The phenotypes caused by loss of *immR* appear to be complicated. The loss of *immR* causes constitutive expression of almost all of the genes in ICE*Bs1* and we suspect that this leads to accumulation of toxic levels of one or more gene products, perhaps components of the ICE*Bs1* mating pore. In addition, loss of *immR* causes increased excision of ICE*Bs1* and the excised element can replicate (J.D. Wang and A.D. Grossman, unpublished data). We suspect that this might also contribute to the cellular phenotypes caused by loss of *immR*.

Identification of the *immR* promoter

immR is transcribed divergently from *xis* (Fig. 1) in a putative operon that also contains *ydcM* (encoding a protein of unknown function) and *int* (encoding the integrase). A fragment containing the *immR* promoter was identified through cloning and functional analysis. We introduced *immR* along with 267 bp of upstream sequence (P*immRimmR*Ω267, Fig. 4A) into an ectopic chromosomal locus in ICE*Bs1*^{0} cells containing a P*xis–lacZ*Ω343 fusion and assayed *xis* expression. *xis* transcription was repressed (Figs 3A and 4B) indicating that this sequence is sufficient for expression of ImmR. Two other constructs that contain *immR* and some upstream sequences were evaluated for the ability to repress transcription of P*xis–lacZ*Ω343. A clone that contained 141 bp upstream of the *immR* open reading frame was able to repress P*xis* (P*immR-immR*Ω141, Fig. 4A and B). In contrast, a clone that contained only 26 bp upstream of the *immR* open reading frame was not able to repress P*xis* (P*spank-immR*Ω26, Fig. 4A and B). This clone contained a functional copy of *immR* because induction of transcription from P*spank* (contained in the clone) established repression (Fig. 3A). These results indicate that there is a functional promoter between 26 and 141 bp upstream of *immR* that is driving expression of *immR*.

Within the sequence between 26 and 141 bp upstream of *immR*, there is an almost perfect match [TG(N)TATTAT, differs from consensus at the underlined position] to the consensus for the extended −10 recognition region for RNA polymerase containing the major sigma subunit, sigma-A (Helmann, 1995). There is not a sequence that is readily recognizable as matching the consensus for the −35 recognition element. Based on the sequence and functional analyses, we conclude that transcription of *immR* most likely initiates from this putative sigma-A-dependent promoter.

ImmR represses and activates its own transcription

We constructed a transcriptional fusion of *lacZ* to the region upstream of and including the 5′ end of the *immR* open reading frame (Fig. 4A). This fusion, P*immR–lacZ*, was expressed at a moderate level in wild-type cells throughout growth (Fig. 4C). Expression was not significantly affected by overexpression of *rapI* or treatment with MMC (data not shown), consistent with previous transcriptional profiling experiments (Auchtung *et al*., 2005).

Expression of the P*immR–lacZ* fusion was decreased >10-fold in the *immR* null mutant or in cells missing ICE*Bs1* entirely (Fig. 4C). These results indicated that ImmR likely activates its own expression.

Complementation of the *immR* null mutation with P*spank-immR* revealed that ImmR both activates and represses transcription from P*immR*, depending on the amount of ImmR (Fig. 4C). When cells were grown in the presence of a high concentration of inducer (1 mM IPTG), P*immR–lacZ* expression was repressed and was about half that in wild-type (ICE*Bs1*$^+$ *immR*$^+$) cells. At a lower concentration of inducer (0.025 mM IPTG), P*immR–lacZ* expression increased approximately threefold relative to that in wild-type cells (ICE*Bs1* $^+$ *immR*$^+$). These results indicate that ImmR activates its own transcription at lower concentrations and represses its own transcription at higher concentrations.

ImmR binds to the *immR-xis* intergenic region

The results described above demonstrated that the promoters for *xis* and *immR* are divergent and located in the *immR-xis* intergenic region, and that these promoters are regulated by ImmR. It seemed likely that ImmR regulates these promoters by binding to sites in this region. To test this, we overexpressed and purified recombinant ImmR-his$_6$ from *Escherichia coli* and tested the ability of this protein to bind to DNA from the intergenic region. Addition of the C-terminal his$_6$ did not disrupt function of ImmR. That is, ImmR-his$_6$ was active *in vivo* as judged by its ability to repress expression of P*xis–lacZ*Ω343 (data not shown). Using mobility shift assays, we found that purified ImmR bound specifically to the DNA from the *xis* and *immR* promoter regions but not to DNA from the *rapI* promoter (data not shown).

We used DNase I protection assays (footprinting) to further characterize the binding of ImmR to the *xis-immR* intergenic region (Figs 5 and 6). We found that at relatively low concentrations (~5–30 nM), ImmR protected six regions in the *xis-immR* intergenic region. We refer to the three regions and the binding sites within these regions that are proximal to *immR* as R1, R2 and R3, and the three regions and sites proximal to *xis* as X1, X2 and X3 (Figs 5 and 6). Three of these six regions were protected at lower concentrations of ImmR (~5–15 nM), whereas the other three regions were protected at somewhat higher concentrations of ImmR (~30 nM) (Fig. 5B and C). Two additional regions were protected at even higher concentrations of ImmR (~100 nM). These protected regions are adjacent to R3 and X1 and labelled ‘a’ and ‘b’ respectively.

The regions protected at lower ImmR concentrations are located between the −10 and −35 of P*xis* (X2), upstream of the −35 of P*xis* (X3), and upstream of the extended −10 of P*immR* (R3). The regions protected at higher ImmR concentrations were downstream of the −10 for P*xis* (X1), downstream of the −10 of P*immR* (R1), and between R1 and R3, adjacent to R3 (R2) (Figs 5 and 6).

We used two motif identification programs, MEME (Bailey and Elkan, 1994) and BIOPROSPECTOR (Liu *et al*., 2001), to search for conserved motifs in these protected regions. We analysed all eight binding regions and also just the six regions with the strongest binding. Based on analysis of the six regions with strongest binding, we identified a 20 bp conserved motif that was present in each protected region (Fig. 6), which is likely the binding sequence for ImmR (Fig. 6). Five of the six binding sites were identified on the same strand of DNA, whereas R2 was on the opposite strand. There is an imperfect inverted repeat contained in this sequence. Inclusion of the two weaker binding regions (a and b) in the sequence analysis resulted in a similar, but more degenerate consensus motif as these putative sites contain several differences from the others. Mutational analyses of all of the proposed sites will be necessary to discern the relative contributions of each to repression from P*xis* and activation and repression from P*immR* and the roles of cooperativity in binding at each site.

Based on their proximities to the sigma-A recognition sequence of P*xis*, we think it is likely that binding of ImmR at X1, X2 and X3 are primarily responsible for repressing transcription of P*xis*. Consistent with this hypothesis, we observed that a shorter P*xis–lacZ* fusion (P*xis–lacZ*Ω136, containing DNA from −136 to −6 bp upstream of the *xis* start codon) that contains X1, X2 and X3, and lacks R1, R2 and R3, was repressed significantly by ImmR, although not to the same level as the P*xis–lacZ*Ω343 fusion containing all six binding sites. Basal expression was three- to fourfold higher in P*xis–lacZ*Ω136 (the shorter fusion) than in P*xis–lacZ*Ω343; both promoter fusions were derepressed to similar levels in response to MMC induction (data not shown). These findings indicate that the region of DNA containing X1, X2 and X3 is primarily responsible for repression of P*xis*. However, additional upstream sequence elements appear to be required for full repression of P*xis*. This

requirement is presumably due to the presence of R1, R2 or R3 and probably involves cooperative interactions with ImmR bound at one or more of these sites.

Activation of the P*immR* promoter does not require X1, X2 or X3, as *immR* is expressed at levels sufficient for P*xis* repression when transcribed from a promoter region that contains only R1, R2 and R3 (Fig. 4A and B). Given the positions of R1, R2 and R3 relative to the sigma-A recognition sequence for P*immR* and the relative affinities of these sites for ImmR *in vitro*, we think it is likely that binding of ImmR to R3 is required for activation of P*immR* and that binding at R1 and R2 may mediate repression. However, it is also possible that repression of P*immR* could involve cooperative interactions between ImmR bound at R1 and/or R2 and X1, X2 or X3. Further work will be needed to distinguish the specific roles for the ImmR-binding sequences and the role of cooperativity.

Identification of other potential sites of ImmR binding

We used the consensus binding motif (Fig. 6) to search the *B. subtilis* genome for additional ImmR binding sites using the Motif Alignment and Search Tool (Bailey and Gribskov, 1998). The *P*-values calculated by MAST for the six ImmR binding sites in the *xis-immR* intergenic region range from 4.1×10^{-9} to 7.1×10^{-8}. Using MAST, we searched for additional sites in the *B. subtilis* chromosome with a *P*-value $\leq 1.0 \times 10^{-7}$. We identified four sites: 1420 bp upstream of *yeeC*, 231 bp upstream of *yhjM* on the strand opposite of its transcription, 808 bp upstream of *fliJ* on the strand opposite of its transcription, and 24 bp upstream of *yonB*. Induction of ICE*Bs1* does not induce expression of any of these genes, nor does the absence or presence of ICE*Bs1* in the genome (data not shown). Therefore, we think it is unlikely that ImmR binding to DNA in these regions significantly influences transcription.

ImmR in recipient cells mediates immunity

We previously observed that acquisition of ICE*Bs1* by conjugal transfer is greatly reduced in cells that already contain the element (Auchtung *et al*., 2005). A similar level of inhibition is observed when excision and transfer is induced by overproduction of RapI or by induction of the DNA damage response (Auchtung *et al*., 2005, and J.M. Auchtung, C.A. Lee, and A.D. Grossman, unpublished results). This seemed similar to the repressor-mediated immunity to superinfection exhibited by various bacteriophage lysogens (Gottesman and Weisberg, 2004; Oppenheim *et al*., 2005).

We found that expression of ImmR in recipient cells inhibits acquisition (i.e. reduces the mating frequency) of ICE*Bs1*. We compared transfer of ICE*Bs1* from donor cells into recipient cells that either did or did not express *immR*. Acquisition of ICE*Bs1* by cells already containing a copy of ICE*Bs1* (expressing *immR* from this element) was ~0.2% of that of cells without a copy of ICE*Bs1* (Table 1, line 1 versus 2). Furthermore, ectopic expression of *immR*, from its own promoter, in cells lacking ICE*Bs1* inhibited acquisition to a similar extent (Table 1, lines 1, 2, 3). These results indicate that production of ImmR in recipient cells is sufficient to confer immunity to acquisition of ICE*Bs1*.

ImmR-mediated immunity can be bypassed by increased levels of Int

In wild-type ICE*Bs1*, *int* appears to be transcribed from the *immR* promoter: *immR*, *ydcM* and *int* are co-oriented and there are no predicted transcriptional terminators present. Thus, the presence of ImmR in mating recipients could potentially limit expression of *int* on the incoming element (by binding to P*immR* and repressing transcription) and prevent acquisition of that element. In addition, ImmR in the recipient could have an effect on some other aspect of ICE*Bs1* function.

We monitored acquisition of ICE*Bs1* in recipients expressing *int*. Expression of *int* (from P*spank*) in recipients lacking ICE*Bs1* had no significant effect on acquisition (Table 1, line 1 versus 5). However, in cells with reduced acquisition due to expression of *immR* (Table 1, line 1 versus 3), expression of *int* restored acquisition to levels similar to those in cells without *immR* (Table 1, line 1, 3, 4). These results indicate that the presence of ImmR in the recipient inhibits expression and/or function of Int and can be bypassed by overproduction of Int.

We also tested for relief of immunity in cells containing ICE*Bs1*Δ*int* and expressing *int* from P*spank*. Expression of *int* in the recipient substantially restored acquisition, but not up levels in cells cured of ICE*Bs1*. Acquisition of the incoming ICE*Bs1* was ~20-fold more efficient than in the absence of ectopic expression of *int* (Table 1, line 6 versus 2), but less efficient (~20-fold) than that of cells cured of ICE*Bs1* (Table 1, line 1). This ~20-fold inhibition of acquisition indicates that there is likely to be another ICE*Bs1*-dependent mechanism that confers immunity independently of the effects of ImmR on Int.

Discussion

Our results show that expression of *immR* in potential recipients is sufficient to confer immunity to acquisition of ICE*Bs1*. More importantly, ImmR promotes stable maintenance of a resident copy of ICE*Bs1* by functioning as a primary regulator of transcription. Inactivation or loss of ImmR, in otherwise ICE*Bs1* $^{+}$ cells, causes increased excision and loss of ICE*Bs1* from host cells (Auchtung *et al*., 2005). ImmR regulates transcription within ICE*Bs1* by binding to sites in the intergenic region shared by the *immR* and *xis* promoters. ImmR represses transcription of genes that mediate excision (*xis*) and transfer and both activates and represses transcription from its own promoter. These properties of ImmR from ICE*Bs1* are similar to those of other repressor proteins from many mobile elements, including the well-studied coliphage lambda (Ptashne, 2004; Dodd *et al*., 2005; Oppenheim *et al*., 2005).

Mechanism of ImmR-mediated immunity

Many mobile genetic elements possess mechanisms to prevent acquisition of additional copies of the same or a related element. One example is superinfection immunity mediated by the lambda repressor CI (reviewed in Echols and Guarneros, 1983; Ptashne, 2004; Oppenheim *et al*., 2005). CI binds to and prevents expression of lytic promoters, thereby preventing lytic development of incoming homoimmune phages. Low levels of *int* expression in an established lysogen also limits the ability of an incoming phage to integrate and form a double lysogen.

ImmR appears to mediate immunity from incoming ICE*Bs1* by limiting production or activity of ICE*Bs1* Int. Expression of *immR* in potential recipients is sufficient to limit acquisition of ICE*Bs1* and this limitation is almost completely suppressed by ectopic expression of *int*. We do not know how ImmR limits production or activity of Int. ImmR activates and represses its own expression, and presumably that of *int* as well. However, there appears to be enough Int produced to allow excision of a resident ICE*Bs1* without further significant increase in *int* mRNA levels (Auchtung *et al*., 2005). Perhaps more Int is needed for integration than for excision. Int could also function preferentially *in cis*, such that the Int that is produced by a resident ICE*Bs1* is much less effective at mediating integration of an incoming element. It is also possible that ImmR somehow inhibits binding of Int to the attachment sites and that increased production of Int overcomes this. If this is the case, then ImmR is likely binding sequences different from the operator sites to which it binds to mediate transcriptional regulation as there are no obvious matches to the consensus operator sequences near the attachment sites.

In addition to limiting stable acquisition of an incoming element, we suspect that ImmR in the recipient will repress transcription from P*xis* on the incoming element, analogous to lambda CI-mediated repression of pL and pR that results in immunity to superinfection. Such repression by ImmR would block expression of *xis* and the downstream conjugation functions, allowing the resident element to remain stably integrated and preventing the incoming element from being transferred to a second recipient.

Our results indicate that there is an additional mechanism or mechanisms contributing to immunity that is independent of the effects of ImmR on Int. ImmR-independent expression of *int* in ICE*Bs1*$^{+}$ cells was not sufficient to restore mating frequencies to the levels observed in cells cured of ICE*Bs1*, as mating occurred ~20-fold less efficiently (Table 1, line 6 versus 1). However, mating into ICE*Bs1*^{0} recipient cells that express *immR* as well as *int* is approximately fourfold less efficient than mating into ICE*Bs1*^{0} recipient cells that express only *int* (Table 1, line 4 versus 5). Therefore, there may be a small Int-independent role for ImmR in mediating immunity as well as other potential immunity mechanisms functioning in ICE*Bs1*.

Based on comparisons to other mobile elements, at least three additional types of regulation seem possible: (i) inhibition of contact between donor and recipient cells (surface exclusion; Achtman *et al*., 1977; Anthony *et al*., 1999), (ii) inhibition of uptake of DNA into the cells (entry exclusion; Achtman *et al*., 1977; Anthony *et al*., 1999), and (iii) inhibition of integration into DNA near an established element (target immunity; Skelding *et al*., 2003, and references therein). Further work will be needed to determine if any of these mechanisms also contribute to ICE*Bs1* immunity and what role, if any, ImmR plays in mediating this regulation.

Organization of the promoter regions regulated by ImmR

The organization of the promoters regulated by ImmR (Fig. 1) is similar to that observed in several bacteriophage, with the promoter for the repressor transcribed divergently from genes involved in lytic development (Lucchini *et al*., 1999; Ptashne, 2004; Waldor and Friedman, 2005). The most well-known of these is bacteriophage lambda. The gene for lambda repressor, *c*I, is transcribed divergently from an operon encoding several genes involved in lytic development (*cro, O, P, Q*) (summarized in Ptashne, 2004). This organization likely contributes to the regulatory circuits that control stability and induction of the integrated element.

Role of autoregulation of *immR*

Autoregulation of *immR* transcription likely serves at least two functions: (i) it maintains the concentration of ImmR at a level high enough to prevent expression of the ICE*Bs1* excision and conjugation genes, and (ii) it maintains ImmR at a level sufficiently low to respond to the appropriate inducing signals.

Similarly, lambda repressor is also autoregulated. CI activates its own transcription at lower concentrations and represses its own transcription at higher concentrations (reviewed in Dodd *et al*., 2005). In the case of lambda, negative autoregulation is needed to maintain low enough concentrations for proper lysogenic induction, whereas positive autoregulation is required to maintain levels of CI sufficient for maintenance of lysogeny (Dodd *et al*., 2005; Michalowski and Little, 2005).

Transcription from P*xis* also appears to be affected by one or more genes in ICE*Bs1* other than *immR*. The existence of the additional regulator(s) is evidenced by the higher levels of ImmR-mediated repression of P*xis* that occur in ICE*Bs1*^{0} cells containing P*immR-immR* expressed ectopically than in wild-type ICE*Bs1*$^{+}$ cells (Figs 3A and 4B). This regulation

could be affecting transcription from P*xis* directly, although we favour the notion that it affects the activity of ImmR. Further work will be needed to determine how additional genes in ICE*Bs1* affect transcription.

Mechanisms of induction of ICE*Bs1*

There are two mechanisms known to activate ICE*Bs1* gene expression and excision, and both are likely to involve relief from ImmR-mediated repression (Auchtung *et al*., 2005). One mechanism involves activation of the RecA-dependent SOS response and the other is independent of RecA and requires RapI. Both mechanisms require at least one other ICE*Bs1* gene product in addition to ImmR (J.M. Auchtung, C.A. Lee and A.D. Grossman, unpubl. results).

Activation of ICE*Bs1* by RapI—RapI is normally produced as cells become crowded and enter stationary phase. Its activity is inhibited by the pentapeptide PhrI that is secreted and then imported via the oligopeptide permease (Auchtung *et al*., 2005). Most of the experiments presented here bypass this regulation due to ectopic overproduction of RapI to induce excision and mating.

Normal production of RapI, when the concentration of PhrI is low, causes increased ICE*Bs1* gene expression and subsequent excision (Auchtung *et al*., 2005). Because both *rapI* and *phrI* are contained in ICE*Bs1*, this regulation normally provides a mechanism for cells to recognize whether neighbours contain ICE*Bs1*. If the neighbours do not contain a copy of ICE*Bs1*, then excision and transfer can occur. Homologues of *rapI* and *phrI* are found in other mobile elements, indicating that this type of recognition of self might be conserved (Auchtung *et al*., 2005).

RapI likely stimulates increased expression of the ICE*Bs1* excision and conjugation genes by inhibiting the activity of ImmR (Auchtung *et al*., 2005). Consistent with this, loss of *immR* is epistatic to loss or overexpression of *rapI* (data not shown). Despite the derepression of P*xis* upon overproduction of RapI, there is little if any obvious effect on transcription from P*immR*, as measured in DNA microarray experiments (Auchtung *et al*., 2005) and in the assays monitoring β-galactosidase activity from a P*immR–lacZ* fusion. In both cases, we were monitoring expression in the bulk population of cells. If *immR* expression had increased in some cells due to loss of ImmR-mediated repression and decreased in other cells due to loss of ImmR-mediated activation, these changes would not have been reflected in our assays. Such effects could be observed by monitoring gene expression in single cells.

In addition, significant derepression of P*xis* occurs at levels of ImmR that still cause transcriptional activation at P*immR* (compare the derepression of P*xis–lacZ*Ω343 expression at 0.025 mM ImmR in Fig. 3A with the increased expression of P*immR–lacZ* at 0.025 mM in Fig. 4C). Therefore, the levels of active ImmR may drop sufficiently low upon overproduction of RapI to allow derepression of P*xis* without losing activation of P*immR*.

Activation of ICE*Bs1* by the SOS response—The RecA-dependent SOS response causes induction of many mobile elements (Walker, 1996; Gottesman and Weisberg, 2004; Dodd *et al*., 2005; McCabe *et al*., 2005; Quinones *et al*., 2005). In many cases, this activation involves the RecA-stimulated autocleavage of a repressor protein. For example, in lambda, activated RecA stimulates autocleavage of CI (Little, 1984) and subsequent derepression of pL and pR, excision, and expression of the lytic pathway (Ptashne, 2004; Oppenheim *et al*., 2005).

In *B. subtilis*, the RecA-dependent SOS response causes induction of expression of ICE*Bs1* genes (Auchtung *et al*., 2005; Goranov *et al*., 2006) and subsequent excision, most likely by causing the inactivation of ImmR (Auchtung *et al*., 2005). This RecA-dependent (RapI-independent) inactivation of ImmR requires at least one other gene in ICE*Bs1* (J.M. Auchtung, C.A. Lee, and A.D. Grossman, unpublished results). This requirement is in marked contrast to the well-characterized mobile elements in which activation of RecA during the SOS response stimulates the autocleavage of the repressor. It will be interesting to characterize the ICE*Bs1* gene responsible for this regulation and to determine its mechanism of action.

Experimental procedures

Media

For standard genetic manipulation, *E. coli* and *B. subtilis* were grown at 37°C in LB (Sambrook and Russell, 2001). For experiments, *B. subtilis* was grown in S7 minimal salts medium (Vasantha and Freese, 1980) (containing 50 mM MOPS instead of 100 mM) with 1% glucose, 0.1% glutamate, with required amino acids as needed [trp and phe (40 μg ml^{-1}), and thr (120 μg ml^{-1})], or LB medium, as indicated. Antibiotics were used at the following concentrations: ampicillin (100 μg ml^{-1}, unless otherwise indicated); chloramphenicol (5 μg ml^{-1}); kanamycin (5 μg ml^{-1}); spectinomycin (100 μg ml^{-1}); streptomycin (100 μg ml^{-1}); and erythromycin (0.5 μg ml^{-1}) and lincomycin (12.5 μg ml^{-1}) together to select for macrolide-lincosamide-streptogramin B (MLS) resistance. IPTG (Sigma) was used at the concentrations indicated, MMC (Sigma) was used at a final concentration of 1 μg ml^{-1}, and L-arabinose (Sigma) was used at a final concentration of 0.2%.

Strains and alleles

Strains used in this study are listed in Table 2. Standard techniques were used for cloning and strain construction (Harwood and Cutting, 1990; Sambrook and Russell, 2001). The BL21-AI (Invitrogen) strain was used for overexpression of *immR-his*$_6$ in *E. coli*. The ICE*Bs1*^{0} strain, the spontaneous streptomycin (*str*) resistant allele (likely in *rpsL*), and the Δ*int205*::*cat*, Δ*immR208*::*cat* and *amyE*::P*spank*(*hy*)-*rapI* alleles were previously described (Auchtung *et al*., 2005). All bp positions are indicated relative to the positions of the start codons annotated in the *B. subtilis* 168 genome sequence.

Δ*int205*::*cat*::*tet* was created by integrating the drug resistance conversion plasmid pCm::Tet (Steinmetz and Richter, 1994) into the Δ*int205*::*cat* allele. Double-cross-over insertion was confirmed by selecting for resistance to tetracycline and screening for sensitivity to chloramphenicol.

P*xis–lacZ*Ω343 (Fig. 2A) was generated by cloning DNA from 343 to 6 bp upstream of the *xis* start codon upstream of a promoterless *lacZ* in the vector pDG793 (Guerout-Fleury *et al*., 1996).

P*immR–lacZ* (Fig. 4A) was generated by cloning the same sequence in the opposite orientation in pDG793. Both vectors were integrated into the chromosome at *thrC* by double-cross-over homologous recombination, which was verified by conversion to threonine auxotrophy.

P*xis–lacZ*Ω136 was generated by cloning DNA from 136 to 6 bp upstream of the *xis* start codon upstream of *lacZ* in pDG793 followed by integration into the chromosome at *thrC* by double-cross-over homologous recombination.

Several fusions to the LacI-repressible IPTG-inducible promoter P*spank* were generated by cloning into the vector pDR110 (Rokop *et al*., 2004). Fusions were then recombined into the chromosome in single copy at *amyE*. P*spank-immR*Ω26 was generated by cloning from −26 to +383 of *immR* into pDR110.

P*spank-int* was generated by cloning −49 to +1128 of *int* into the pCAL215, which contains *lacI*, P*spank*, and the multiple cloning site from pDR110, ligated into the *thrC* integration vector pDG795 (Guerout-Fleury *et al*., 1996). This vector was integrated into the chromosome by double-cross-over homologous recombination, which was verified by conversion to threonine auxotrophy.

P*immR-immR*Ω141 was generated by cloning from −141 to +383 of *immR* into pDR110. *immR* was under control of its own promoter and P*spank*. Expression of *immR* from this construct occurred independently of IPTG.

P*immR-immR*Ω267 was generated by cloning the sequence from −267 of *immR* to +383 of *immR* into the integration vector, pMMB124, which was a generous gift from M.B. Berkmen. pMMB124 contains segments of *cgeD* flanking the kanamycin resistance gene in pGK67 (Lemon *et al*., 2001). This allows for integration of DNA by double-cross-over homologous recombination into *cgeD*. Double-cross-over integrants were identified by screening for sensitivity to chloramphenicol, which is encoded on the plasmid backbone outside of the *cgeD* regions.

immR-his$_6$ was created by cloning the *immR* coding sequence (+1 to +380) along with an optimized ribosome-binding sequence (*rbs*) and spacer region (AGGAGGAAAAACAT, *rbs* is underlined) downstream of the T7 promoter in the pET21-*cat* vector to create plasmid pJMA605. pET21-*cat* contains the chloramphenicol resistance gene from pJH101 (Ferrari *et al*., 1983) in the SphI site of pET21 (Novagen). pJMA605 was introduced into the *B. subtilis* chromosome by single-cross-over homologous recombination to generate *immR:immR-his*$_6$ *cat*.

β-Galactosidase assays

β-Galactosidase-specific activity was determined as described (Jaacks *et al*., 1989). Specific activity was calculated relative to the optical density at 600 nm (OD_{600}) of thesamples. Results shown are from single experiments that are representative of results observed in at least two independent experiments.

Excision assays

Qualitative assays—Total DNA was prepared using Qiagen DNeasy Tissue Kit as described (Auchtung *et al*., 2005). PCR reactions were performed using the previously described primers and conditions (Auchtung *et al*., 2005), using 100 ng of DNA as a template in each reaction. PCR products were visualized by electrophoresis on 2% agarose gels stained with Ethidium bromide. Gel images were captured with the ChemiImager gel documentation system (Alpha Innotech).

Quantitative assay—Quantitative PCR reactions were performed as described, using twofold dilutions of template to obtain PCR products amplified in the linear range (Auchtung *et al*., 2005). Gel images were captured and spot densitometry was performed with the ChemiImager gel documentation system (Alpha Innotech). In order to determine the percentage of cells in which excision had occurred, the ratio of the PCR signal from repaired chromosomal junction as a fraction of the PCR signal from a control site for the experimental sample (wild type or Δ*immR*) was normalized to the ratio of repaired

chromosomal junction to the control site in cells lacking ICE*Bs1* (JMA222), which simulates 100% excision. The repaired chromosomal junction was used rather than the circular ICE*Bs1* excision product to avoid overestimates due to replication of the excised product.

Mating assays

Donor and recipient cells were grown in LB medium. Matings were performed on filter paper essentially as described (Auchtung *et al*., 2005). Briefly, IPTG (1 mM) was added to donor cells in mid-exponential growth (OD_{600} ~ 0.2) to induce expression of P*spank*(*hy*)-*rapI*; RapI then causes induction of ICE*Bs1* gene expression and excision. One hour after expression of RapI, donors were mixed with recipients, filtered to allow mating, and transconjugants were identified and mating frequencies were calculated. Recipient cells containing P*spank-int* were grown in the presence of IPTG (1 mM).

Primer extension assays

The 5′ end of the *xis* transcript was determined by primer extension analysis. RNA was isolated using the RNeasy kit from Qiagen according to the manufacturer's protocol. Ten micrograms of RNA from untreated wild-type cells, wild-type cells treated with MMC, and cells overexpressing *rapI* was reverse transcribed as described (Auchtung *et al*., 2005), except that ~2 pmol of specific ^{32}P-labelled oligonucleotide was used as a primer. Oligonucleotides oJMA102, complementary to −6 to −17 relative to the *xis* start codon, and oJMA240, complementary to +22 to +49 of *xis*, were end-labelled with [γ-^{32}P]-ATP (Perkin-Elmer) using T4 polynucleotide kinase (New England Biolabs). Labelled oligonucleotides were separated from unincorporated ATP using Qiagen's Nucleotide Removal Kit. Products of the primer extension reactions were compared with the products of dideoxynucleotide sequencing reactions performed with the fmol DNA Cycle Sequencing System (Promega) using labelled oJMA102 or oJMA240 as primers and PCR products corresponding to −6 to −131 or +22 to −131 of *xis* as template. Primer extension and dideoxynucleotide sequencing reactions were electrophoresed on 6% polyacrylamide 7 M urea gels. Radioactivity was detected through phosphorimaging using the Typhoon imager 9400 (Amersham Biosciences).

Purification of ImmR-his$_6$

Escherichia coli BL21 cells containing an arabinose-inducible copy of the T7 RNA polymerase (BL21-AI, Invitrogen) and a plasmid encoding *immR-his*$_6$ under the control of a LacI-repressible/IPTG-inducible T7 polymerase-dependent promoter were grown in LB (containing 200 mg ml^{-1} ampicillin) at 37°C with shaking. At OD_{600} ~ 0.4, L-arabinose and 1 mM IPTG were added to induce expression of the T7 polymerase and derepress expression of *immR-his*$_6$. One hundred millilitres of cells were collected 4 h after induction, pelleted by centrifugation, decanted and stored at −80°C.

The cell pellet was thawed on ice, re-suspended in 0.2 volumes lysis buffer (50 mM NaH_2PO_4, 300 mM NaCl, 10 mM imidazole, pH 8.0) and lysed by sonication on ice for 4 × 30 s. Supernatant was separated by centrifugation at 10 000 *g* at 4°C for 20 min. ImmR-his$_6$ was purified by Ni-NTA column chromatography (Qiagen) according to the manufacturer's protocol for batch purification under native conditions, except that proteins were eluted by increased imidazole concentrations (50, 100, 200 and 400 mM imidazole).

Elution fractions were analysed by SDS-PAGE. ImmR was present in the 400 mM elution fraction and was ~95% pure. ImmR was dialysed into buffer (50 mM NaH_2PO_4, 300 mM NaCl, pH 8.0) at 4°C overnight, glycerol was added to 50% and concentration was determined by Bradford assay (Bio-Rad). Protein was stored at −80°C.

DNase I protection assays

DNA fragments from the *xis-immR* intergenic region were labelled at one end using ^{32}P-labelled primers oJMA109 or oJMA240 in PCR reactions along with an unlabelled primer (oJMA240 or oJMA109). Labelled PCR products were purified on polyacrylamide gels and eluted into buffer containing 0.5 M ammonium acetate, 10 mM magnesium acetate and 2 mM EDTA at 37°C overnight. Labelled DNA was ethanol-precipitated and re-suspended in buffer (10 mM Tris-HCl, 20 mM NaCl, 0.1 mM EDTA pH 8).

ImmR-his$_6$ (1–200 nM) was allowed to bind the labelled DNA (≤ 0.4 μM) in binding buffer (20 mM Tris-HCl, 50 mM KCl, 3 mM $MgCl_2$, 5% glycerol, 2.5 mM $CaCl_2$, 50 ng μl^{-1} poly (dI/dC), 100 ng μl^{-1} BSA, pH 7.5) in 25 μl of reactions at 37°C for 10 min, followed by incubation at room temperature incubation for 20 min. DNase I (0.5 units) (Ambion) was added to each reaction (total reaction volume = 30 μl), and incubated for 1 min at room temperature prior to the addition of 7.5 μl of stop solution (3.3% SDS, 60 mM EDTA, 0.5 mM Tris-HCl pH 9.5).

DNA was isolated from each reaction by phenol-chloroform extraction followed by ethanol precipitation in the presence of yeast tRNA as carrier and 3 mM sodium acetate. DNA was re-suspended in 3 μl of buffer (10 mM Tris, 10 mM EDTA, pH 8). An equal volume of formamide running buffer (90% formamide, 10 mM EDTA, 0.04% xylene cyanol, 0.04% bromphenol blue) was added to each sample.

In order to determine which regions were protected from DNase I digestion by ImmR binding, dideoxynucleotide sequencing reactions of the *xis-immR* intergenic region were also performed (as described above) using the corresponding radiolabelled primer (oJMA109 or oJMA240). DNase I protection and dideoxynucleotide sequencing reactions were analysed by electrophoresis on 6% polyacrylamide 7 M urea gels. Radioactivity was detected through phosphorimaging using the Typhoon imager 9400 (Amersham Biosciences).

Acknowledgments

We thank M.B. Berkmen for providing plasmid pMMB124, K. MacIsaac for advice about motif searching, and A.L. Sonen-shein, F. Solomon, G. Walker, R. Sauer and J.D. Wang for comments on the manuscript. This work was supported in part by Public Health Service Grant GM50895 from the NIH to A.D.G.

References

Achtman M, Kennedy N, Skurray R. Cell–cell interactions in conjugating *Escherichia coli*: role of *traT* protein in surface exclusion. Proc Natl Acad Sci USA. 1977; 74:5104–5108. [PubMed: 337311]

Anthony KG, Klimke WA, Manchak J, Frost LS. Comparison of proteins involved in pilus synthesis and mating pair stabilization from the related plasmids F and R100-1: insights into the mechanism of conjugation. J Bacteriol. 1999; 181:5149–5159. [PubMed: 10464182]

Auchtung JM, Lee CA, Monson RE, Lehman AP, Grossman AD. Regulation of a *Bacillus subtilis* mobile genetic element by intercellular signaling and the global DNA damage response. Proc Natl Acad Sci USA. 2005; 102:12554–12559. [PubMed: 16105942]

Bailey TL, Elkan C. Fitting a mixture model by expectation maximization to discover motifs in biopolymers. Proc Int Conf Intell Syst Mol Biol. 1994; 2:28–36. [PubMed: 7584402]

Bailey TL, Gribskov M. Combining evidence using p-values: application to sequence homology searches. Bioinformatics. 1998; 14:48–54. [PubMed: 9520501]

Brussow H, Canchaya C, Hardt WD. Phages and the evolution of bacterial pathogens: from genomic rearrangements to lysogenic conversion. Microbiol Mol Biol Rev. 2004; 68:560–602. [PubMed: 15353570]

Burrus V, Waldor MK. Shaping bacterial genomes with integrative and conjugative elements. Res Microbiol. 2004; 155:376–386. [PubMed: 15207870]

Burrus V, Pavlovic G, Decaris B, Guedon G. The ICE*St1* element of *Streptococcus thermophilus* belongs to a large family of integrative and conjugative elements that exchange modules and change their specificity of integration. Plasmid. 2002; 48:77–97. [PubMed: 12383726]

Crooks GE, Hon G, Chandonia JM, Brenner SE. WebLogo: a sequence logo generator. Genome Res. 2004; 14:1188–1190. [PubMed: 15173120]

Dodd IB, Shearwin KE, Egan JB. Revisited gene regulation in bacteriophage lambda. Curr Opin Genet Dev. 2005; 15:145–152. [PubMed: 15797197]

Echols, H.; Guarneros, G. Control of integration and excision. In: Hendrix, RW.; Roberts, JW.; Stahl, FW.; Weisberg, RA., editors. Lambda II. Cold Spring Harbor, NY: Cold Spring Harbor Laboratory Press; 1983. p. 75-92.

Ferrari FA, Nguyen A, Lang D, Hoch JA. Construction and properties of an integrable plasmid for *Bacillus subtilis*. J Bacteriol. 1983; 154:1513–1515. [PubMed: 6304019]

Frost LS, Leplae R, Summers AO, Toussaint A. Mobile genetic elements: the agents of open source evolution. Nat Rev Microbiol. 2005; 3:722–732. [PubMed: 16138100]

Goranov AI, Kuester-Schoeck E, Wang JD, Grossman AD. Characterization of the global transcriptional responses to different types of DNA damage and disruption of replication in *Bacillus subtilis*. J Bacteriol. 2006; 188:5595–5605. [PubMed: 16855250]

Gottesman ME, Weisberg RA. Little lambda, who made thee? Microbiol Mol Biol Rev. 2004; 68:796–813. [PubMed: 15590784]

Guerout-Fleury AM, Frandsen N, Stragier P. Plasmids for ectopic integration in *Bacillus subtilis*. Gene. 1996; 180:57–61. [PubMed: 8973347]

Harwood, CR.; Cutting, SM. Molecular Biological Methods for Bacillus. Chichester: John Wiley & Sons; 1990.

Helmann JD. Compilation and analysis of *Bacillus subtilis* sigma A-dependent promoter sequences: evidence for extended contact between RNA polymerase and upstream promoter DNA. Nucleic Acids Res. 1995; 23:2351–2360. [PubMed: 7630711]

Jaacks KJ, Healy J, Losick R, Grossman AD. Identification and characterization of genes controlled by the sporulation-regulatory gene *spo0H* in *Bacillus subtilis*. J Bacteriol. 1989; 171:4121–4129. [PubMed: 2502532]

Jarmer H, Larsen TS, Krogh A, Saxild HH, Brunak S, Knudsen S. Sigma A recognition sites in the *Bacillus subtilis* genome. Microbiology. 2001; 147:2417–2424. [PubMed: 11535782]

Lemon KP, Kurtser I, Grossman AD. Effects of replication termination mutants on chromosome partitioning in *Bacillus subtilis*. Proc Natl Acad Sci USA. 2001; 98:212–217. [PubMed: 11134515]

Little JW. Autodigestion of LexA and phage lambda repressors. Proc Natl Acad Sci USA. 1984; 81:1375–1379. [PubMed: 6231641]

Liu, X.; Brutlag, DL.; Liu, JS. BioProspector: discovering conserved DNA motifs in upstream regulatory regions of co-expressed genes. In: Altman, RB.; Dunker, RK.; Hunter, L.; Lauderdale, K.; Klein, TE., editors. Pacific Symposium on Biocomputing. Hackensack, N.J: World Scientific Press; 2001. p. 127-138.

Lucchini S, Desiere F, Brussow H. Similarly organized lysogeny modules in temperate Siphoviridae from low GC content gram-positive bacteria. Virology. 1999; 263:427–435. [PubMed: 10544115]

McCabe BC, Pawlowski DR, Koudelka GB. The bacteriophage 434 repressor dimer preferentially undergoes autoproteolysis by an intramolecular mechanism. J Bacteriol. 2005; 187:5624–5630. [PubMed: 16077107]

McQuade RS, Comella N, Grossman AD. Control of a family of phosphatase regulatory genes (*phr*) by the alternate sigma factor sigma-H of *Bacillus subtilis*. J Bacteriol. 2001; 183:4905–4909. [PubMed: 11466295]

Michalowski CB, Little JW. Positive autoregulation of *c*I is a dispensable feature of the phage lambda gene regulatory circuitry. J Bacteriol. 2005; 187:6430–6442. [PubMed: 16159777]

Ochman H, Lawrence JG, Groisman EA. Lateral gene transfer and the nature of bacterial innovation. Nature. 2000; 405:299–304. [PubMed: 10830951]

Oppenheim AB, Kobiler O, Stavans J, Court DL, Adhya S. Switches in bacteriophage lambda development. Annu Rev Genet. 2005; 39:409–429. [PubMed: 16285866]

Perego M, Spiegelman GB, Hoch JA. Structure of the gene for the transition state regulator, *abrB*: regulator synthesis is controlled by the *spo0A* sporulation gene in *Bacillus subtilis*. Mol Microbiol. 1988; 2:689–699. [PubMed: 3145384]

Ptashne, M. A Genetic Switch: Phage Lambda Revisited. Cold Spring Harbor, NY: Cold Spring Harbor Laboratory Press; 2004.

Quinones M, Kimsey HH, Waldor MK. LexA cleavage is required for CTX prophage induction. Mol Cell. 2005; 17:291–300. [PubMed: 15664197]

Rokop ME, Auchtung JM, Grossman AD. Control of DNA replication initiation by recruitment of an essential initiation protein to the membrane of *Bacillus subtilis*. Mol Microbiol. 2004; 52:1757–1767. [PubMed: 15186423]

Sambrook, J.; Russell, DW. Molecular Cloning: A Laboratory Manual. Cold Spring Harbor, NY: Cold Spring Harbor Laboratory Press; 2001.

Skelding Z, Queen-Baker J, Craig NL. Alternative interactions between the Tn*7* transposase and the Tn*7* target DNA binding protein regulate target immunity and transposition. EMBO J. 2003; 22:5904–5917. [PubMed: 14592987]

Steinmetz M, Richter R. Plasmids designed to alter the antibiotic resistance expressed by insertion mutations in *Bacillus subtilis*, through *in vivo* recombination. Gene. 1994; 142:79–83. [PubMed: 8181761]

Vasantha N, Freese E. Enzyme changes during *Bacillus subtilis* sporulation caused by deprivation of guanine nucleotides. J Bacteriol. 1980; 144:1119–1125. [PubMed: 6777366]

Waldor MK, Friedman DI. Phage regulatory circuits and virulence gene expression. Curr Opin Microbiol. 2005; 8:459–465. [PubMed: 15979389]

Walker, GC. The SOS response of *Escherichia coli*. In: Neidhardt, FC.; Curtiss, R., III; Ingraham, JL.; Lin, EC.; Low, KB.; Magasanik, B., et al., editors. Escherichia coli and Salmonella: Cellular and Molecular Biology. Washington, DC: American Society for Microbiology; 1996. p. 1400-1416.

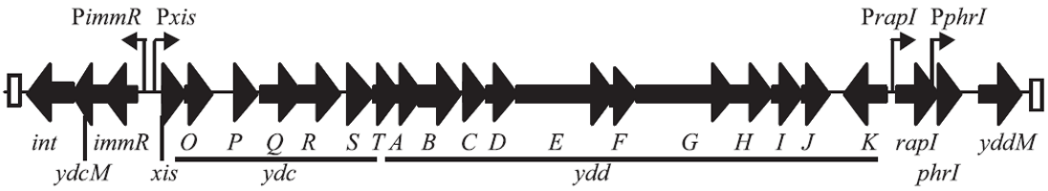

Fig. 1. Organization of open reading frames in ICE*Bs1*

The 24 open reading frames of ICE*Bs1* are indicated by thick black arrows, oriented in the direction of transcription, with the name of each gene indicated below the arrow. *ydcO-ydcT* and *yddA-yddK* are indicated by the terminal unique letter directly under each arrow and the appropriate initial three-letter designation indicated underneath each underlined section of arrows. *ydc* and *ydd* indicate genes with unknown function. The positions of the promoters for *xis, immR, rapI* (Jarmer *et al*., 2001; Auchtung *et al*., 2005) and *phrI* (McQuade *et al*., 2001) are indicated by vertical lines with small arrows pointed in the direction of transcription. The 60 bp direct repeats marking the ends of the element are indicated by white boxes.

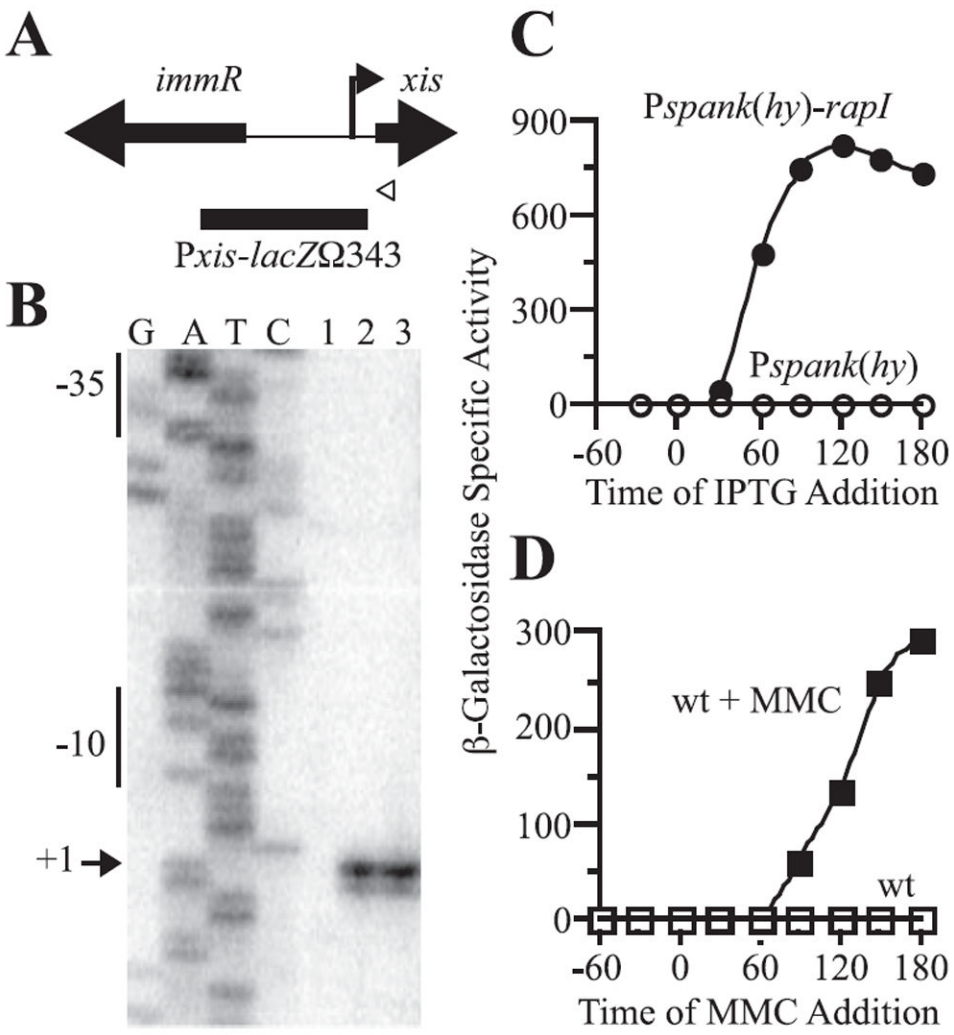

Fig. 2. Characterization of the *xis* promoter and its activation by RapI overexpression and the global DNA damage response

A. Schematic of *xis*, *immR*, and the shared intergenic region. The thick arrows indicate the locations of the *xis* and *immR* genes, and show the orientation of transcription of each. The white arrowhead indicates the position of the primer used for the primer extension assay in (B). The 5′ end of the *xis* transcript identified in (B) is indicated by a vertical line and arrow pointing to the right. The black box indicates the region upstream of *xis* fused to *lacZ* and used to monitor *xis* expression in (C) and (D).

B. The 5′ end of the *xis* transcripts was determined by primer extension assays. G, A, T and C indicate the lanes containing dideoxynucleotide sequencing reactions with the indicated nucleotide. RNA was isolated from untreated wild-type cells (JH642, lane 1); from wild-type cells 1 h after treatment with mitomycin C (lane 2); and from P*spank*(*hy*)-*rapI* cells (JMA28) 30 min after treatment with IPTG (lane 3). Results of reverse transcription reactions with the primer indicated in (A) are shown; similar results were seen when reverse transcription reactions were carried out with a primer more proximal to +1 (data not shown). The sequences complementary to the consensus −10 and −35 regions are indicated on the left of the gel. The arrow indicates the nucleotide complementary to the end of the major transcript.

C and D. Cells containing a P*xis–lacZ*Ω343 fusion were grown in minimal medium and samples for β-galactosidase assays were collected at the times indicated. Cells were treated with 1 mM IPTG (C) or 1 μg ml^{-1} MMC (D) in mid-exponential phase (OD_{600} = 0.4–0.6). β-Galactosidase-specific activities were calculated relative to the cell densities (OD_{600}) of the cultures. β-Galactosidase-specific activities are plotted relative to the time (in minutes) before and after addition of IPTG or MMC. In these graphs, β-galactosidase specific activity in wild-type cells appears to be at or near background (zero) levels. However, there is a low level of activity above background (Fig. 3A and B).

C. *xis* expression in cells (KLG126) containing P*xis–lacZ*Ω343 and P*spank*(*hy*)-*rapI* (●) and cells (KLG125) containing P*xis–lacZ*Ω343 and P*spank*(*hy*) empty vector (○).

D. *xis* expression in P*xis–lacZ*Ω343 cells (JMA201) (□) and P*xis–lacZ*Ω343 cells treated with MMC (■).

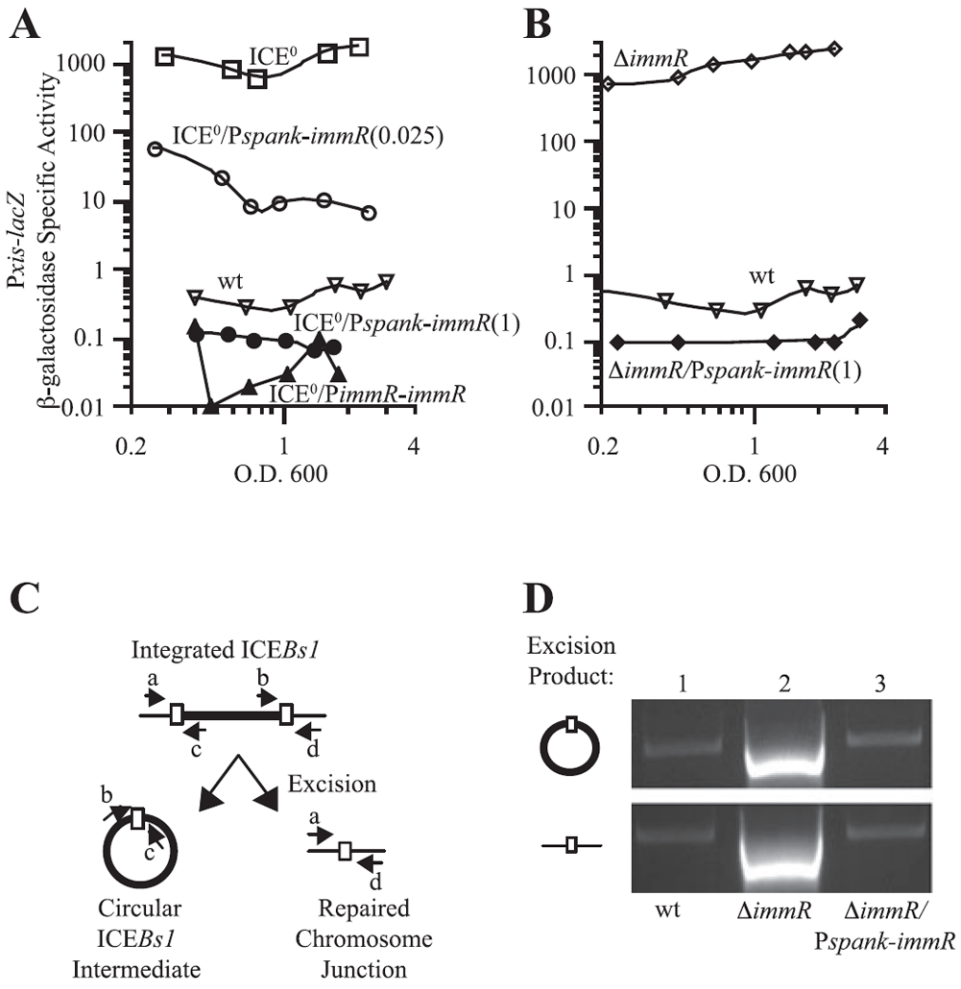

Fig. 3. ImmR regulates excision through transcription of *xis*

A and B. P*xis*–*lacZ*Ω343 expression was monitored throughout exponential growth in minimal medium as described in Fig. 2. IPTG (0.025 or 1 mM, as indicated) was present throughout growth.

A. P*xis*–*lacZ*Ω343 expression in wild-type (ICE*Bs1*$^{+}$) cells (JMA201, ▽, wt); ICE*Bs1*^{0} (JMA264, □, ICE^{0}); ICE*Bs1*^{0} P*spank-immR*Ω26 (JMA362) cells grown in the presence of 0.025 mM [○, ICE^{0}/P*spank-immR*(0.025)] or 1 mM IPTG [●, ICE^{0}/P*spank-immR*(1)]; and ICE*Bs1*^{0} P*immR-immR*Ω267 (JMA421, ▲, ICE^{0}/P*immR-immR*) cells.

B. P*xis*–*lacZ*Ω343 expression in wild-type cells (JMA201, ▽, wt; same data as in A); Δ*immR* cells (JMA214, ◊, Δ*immR*); and Δ*immR* P*spank-immR*Ω26 cells in the presence of 1 mM IPTG (JMA541, ◆, Δ*immR*/P*spank-immR*).

C. Schematic representation of the excision assay performed in (D). Upon excision of ICE*Bs1* from the chromosome, two products are formed, an ICE*Bs1* circular intermediate and a repaired chromosomal junction. These products can be detected through PCR using primers b + c and a + d (respectively), which are represented by small arrows in the diagram. The sequences of these primers [oJMA93 (a), oJMA95 (b), oJMA97 (c) and oJMA100 (d)] were described previously (Auchtung *et al*., 2005).

D. Excision was monitored in wild-type (JMA201, lane 1), Δ*immR* (JMAM214, lane 2) and Δ*immR* P*spank-immR*Ω26 (JMA541, grown in the presence of 1 mM IPTG, lane 3) cells. DNA was extracted from cells in exponential phase and 100 ng was used as template to

amplify the indicated products described in (C). Quantitative PCR performed on DNA extracted from a population of Δ*immR* cells revealed that excision occurred in ~97% of cells whereas excision occurred in ~0.003% of wild-type cells.

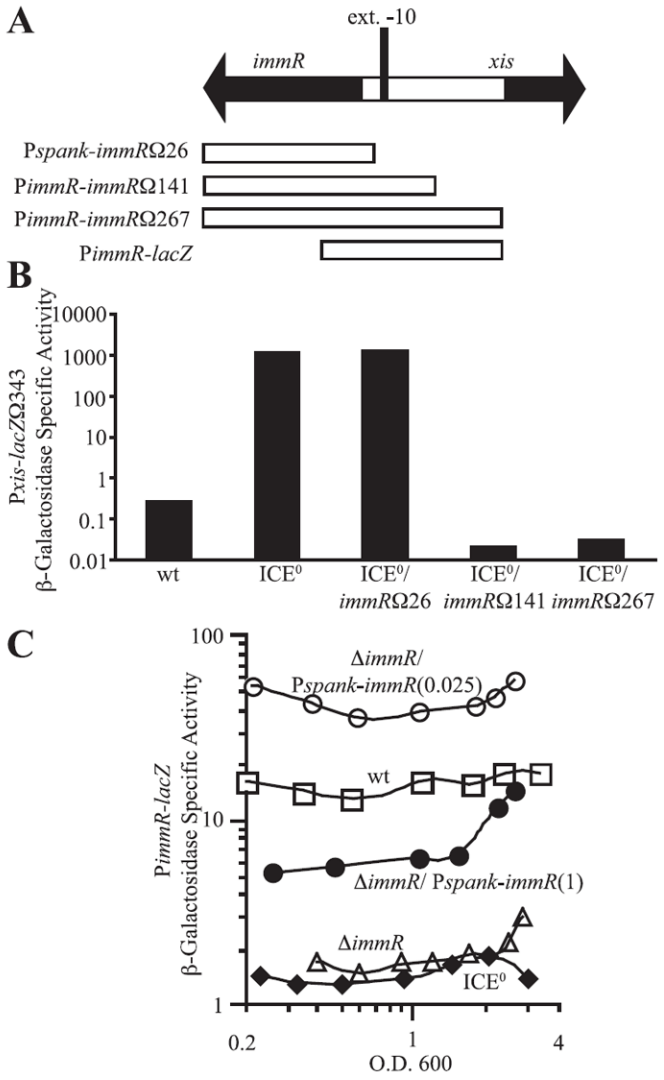

Fig. 4. ImmR represses and activates its own transcription

A. Schematic of *xis*, *immR*, and the intergenic region. *xis*, *immR*, and their direction of transcription are indicated by the large black arrows. The location of the putative extended −10 recognition sequence for $E\sigma^A$ is indicated by a vertical black rectangle (ext. −10). The sequences present in the *immR* constructs used in (B) and (C) are indicated by white boxes underneath the diagram.

B. Functional analysis of the *immR* promoter. Constructs containing the entire *immR* open reading frame and segments of its upstream sequence (diagrammed in A) were tested for their ability to reconstitute ImmR function by repressing transcription of P*xis–lacZ*Ω343 in ICE*Bs1*^{0} cells. β-Galactosidase-specific activity in cells grown to mid-late exponential phase (OD_{600} ~ 1) in minimal medium was determined. P*xis–lacZ*Ω343 containing cells assayed were wild type (JMA201, wt); ICE*Bs1*^{0} (JMA264, ICE^0); ICE*Bs1*^{0} P*spank-immR*Ω26 (JMA362, ICE^0/*immR*Ω26); ICE*Bs1*^{0} P*immR-immR*Ω141 (JMA266, ICE^0/*immR*Ω141); and ICE*Bs1*^{0} P*immR-immR*Ω267 (JMA421, ICE^0/*immR*Ω267).

C. Expression of a P*immR–lacZ* fusion was monitored throughout exponential growth in minimal medium in otherwise wild-type cells (JMA309, □), Δ*immR* (JMA310, Δ), ICE*Bs1*^{0} (JMA576, ◆) and Δ*immR* P*spank-immR*Ω26 cells (JMA638) grown in the in the presence

of 0.025 (○) or 1 mM IPTG (●). IPTG, when used, was present throughout growth. β-Galactosidase-specific activities are plotted relative to the OD_{600} of the cultures.

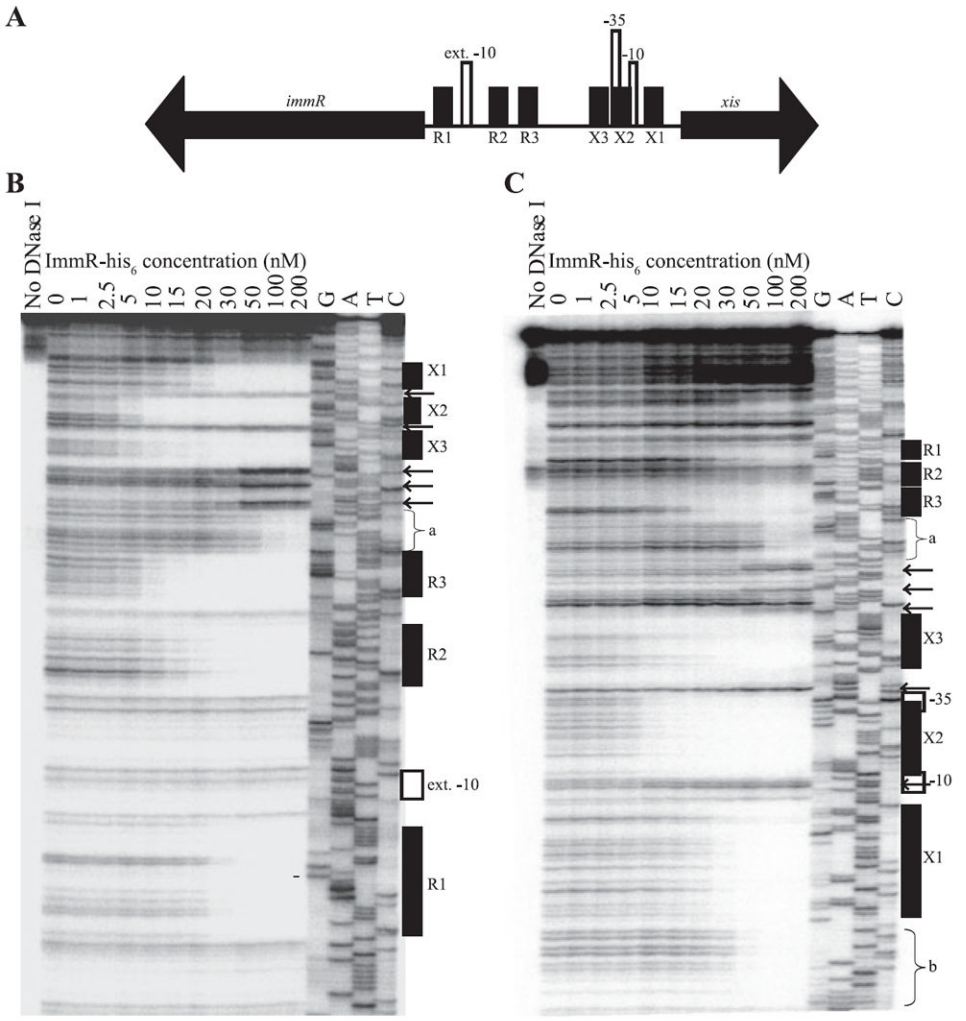

Fig. 5. ImmR binds to the *xis* and *immR* intergenic region

A. Detailed schematic of *xis*, *immR*, and the intergenic region. *xis*, *immR*, and the directions of transcription are indicated by the big black arrows. The location of the putative extended −10 recognition sequence for sigma-A-containing RNA polymerase in the *immR* promoter, and the −10 and −35 recognition sequences for sigma-A-containing RNA polymerase in the *xis* promoter are indicated by vertical white rectangles. The positions of the six regions protected by ImmR (sites X1, X2, X3, R1, R2 and R3) are indicated by shorter vertical black boxes.

B and C. Binding of ImmR to the *xis*-*immR* intergenic region was monitored through DNase I protection assays. Increasing concentrations (1–200 nM) of purified ImmR-his6 protein were incubated with radiolabelled DNA from the *xis*-*immR* intergenic region. DNase I was added to each reaction to digest DNA not protected by ImmR. Reactions were analysed by electrophoresis along with dideoxynucleotide sequencing reactions of the *xis*-*immR* intergenic region. The concentrations of ImmR used in each reaction are indicated above each lane of the gel. G, A, T and C indicate the dideoxynucleotide used in each sequencing reaction. Positions of the extended −10 recognition sequence for $E\sigma^A$ in the *immR* promoter, and the −10 and −35 recognition sequences for $E\sigma^A$ in the *xis* promoter, the six protected regions described in (A), and the two additional sites of ImmR protection (a and b) are indicated to the right of each gel image. The arrows indicate the positions of DNase I

hypersensitive sites. In (B), the 5′ end of DNA at the *immR* end (the top strand) was labelled; in (C), the 5′ end of DNA near *xis* (the bottom strand) was labelled.

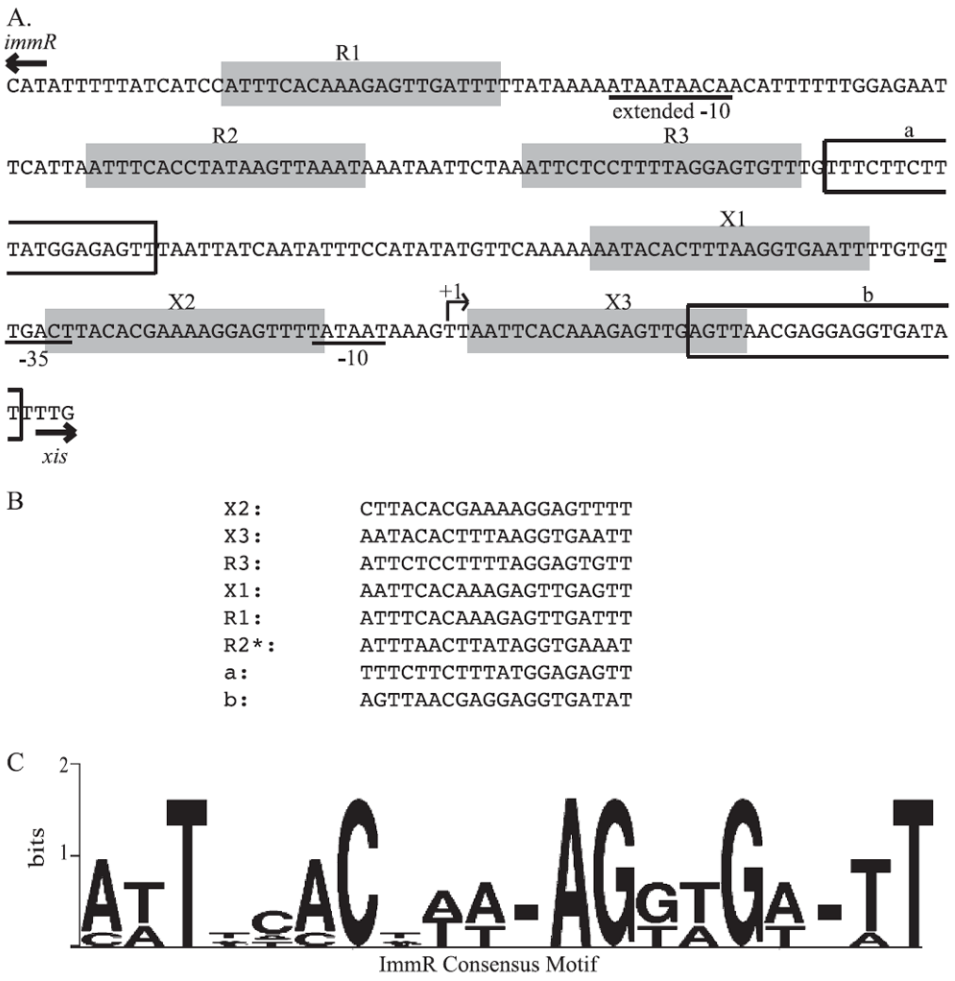

Fig. 6. Identification of a conserved ImmR binding motif

A. The sequence of a single strand of the *xis-immR* intergenic region is shown. The positions of the *immR* and *xis* start codons are indicated by arrows above the appropriate sequences. The positions of the P*immR* extended −10 and the P*xis* −35 and −10 recognition sequences for RNA polymerase containing sigma-A are indicated by the underlined nucleotides. The positions of R1, R2 and R3, and X1, X2 and X3 are indicated by grey boxes. R1, R3, and X1, X2 and X3 are all on the same strand of DNA whereas R2 is on the complementary strand. The positions of the a and b sites are indicated by white boxes.

B. An alignment of the nucleotide sequences of all eight sites protected by ImmR listed in order of ImmR affinities observed in the DNase I protection experiments (Fig. 5).

C. A representation of the consensus motif for the ImmR-binding sequence was generated using Weblogo (Crooks *et al*., 2004). The size of each nucleotide corresponds to the frequency with which that nucleotide was observed in that position; dashes at a position indicate lack of consensus.

Table 1

ImmR inhibits acquisition of ICE*Bs1* by recipient cells and is bypassed by expression of *int*.

Recipient[a] (strain No.)	Mating frequency[b]
1. ICE*Bs1*^{0} (CAL419)	$(5.1 \pm 2.4) \times 10^{-3}$
2. ICE*Bs1*$^+$ (JMA875)	$(9.2 \pm 4.0) \times 10^{-6}$
3. ICE*Bs1*^{0}; P*immR-immR* (JMA872)	$(2.4 \pm 0.62) \times 10^{-6}$
4. ICE*Bs1*^{0}; P*immR-immR*; P*spank-int* (JMA873)	$(2.0 \pm 0.84) \times 10^{-3}$
5. ICE*Bs1*^{0}; P*spank-int* (JMA878)	$(8.0 \pm 2.3) \times 10^{-3}$
6. ICE*Bs1*(Δ*int*); P*spank-int* (JMA882)	$(2.2 \pm 0.78) \times 10^{-4}$

[a] All recipients contained a *comK* null mutation and were streptomycin resistant (*str*). Recipient cells containing P*spank-int* were grown in the presence of IPTG to allow production of Int.

[b] Mating assays were performed as described (Auchtung *et al*., 2005). The mating frequency is the mean number of transconjugants per donor cell (±standard error of the mean), calculated from at least two experiments. The donor strain was JMA168 [ICE*Bs1*(Δ*rapIphrI*::*kan*); P*spank*(*hy*)-*rapI*]. Expression of P*spank*(*hy*)-*rapI* was induced with IPTG 1 h before mating. Production of RapI causes excision of ICE*Bs1* and expression of its conjugation genes.

Table 2

Strains used in this study.

Strain	Relevant genotype[a]
JH642	*trpC2 pheA1*
CAL419	ICE*Bs1*^{0} *comK*::*cat str*
JMA28	*amyE*::[(P*spank*(*hy*)-*rapI*) *spc*]
JMA168	Δ(*rapI-phrI*)*342*::*kan amyE*::[(P*spank*(*hy*)-*rapI*) *spc*]
JMA201	*thrC*::[(P*xis–lacZ*Ω343) *erm*]
JMA214	Δ*immR208*::*cat thrC*::[(P*xis–lacZ*Ω343) *erm*]
JMA264	ICE*Bs1*^{0} *thrC*::[(P*xis–lacZ*Ω343) *erm*]
JMA266	ICE*Bs1*^{0} *amyE*::[(P*immR-immR*Ω141) *spc*] *thrC*::[(P*xis–lacZ*Ω343) *erm*]
JMA309	*thrC*::[(P*immR–lacZ*) *erm*]
JMA310	Δ*immR208*::*cat thrC*::[(P*immR–lacZ*) *erm*]
JMA362	ICE*Bs1*^{0} *amyE*::[(P*spank-immR*Ω26) *spc*] *thrC*::[(P*xis–lacZ*Ω343) *erm*]
JMA421	ICE*Bs1*^{0} *cgeD*::[(P*immR-immR*Ω267) *kan*] *thrC*::[(P*xis–lacZ*Ω343) *erm*]
JMA541	Δ*immR208*::*cat amyE*::[(P*spank-immR*Ω26) *spc*] *thrC*::[(P*xis–lacZ*Ω343) *erm*]
JMA576	ICE*Bs1*^{0} *thrC*::[(P*immR–lacZ*) *erm*]
JMA631	ICE*Bs1*^{0} *cgeD*::[(P*immR-immR-his*$_6$ *cat*) *kan*] *thrC*::[(P*xis–lacZ*Ω343) *erm*]
JMA638	Δ*immR208*::*cat amyE*::[(P*spank-immR*Ω27) *spc*] *thrC*::[(*immR–lacZ*) *erm*]
JMA683	*thrC*::[(P*xis–lacZ*Ω136) *erm*]
JMA870	ICE*Bs1*^{0} *cgeD*::[(P*spank*(*hy*)-*rapI*) *kan*] *thrC*::[(P*xis–lacZ*Ω343) *erm*]
JMA872	ICE*Bs1*^{0} *amyE*::[(P*immR-immR*Ω141) *spc*] *comK*::*cat str*
JMA873	ICE*Bs1*^{0} *amyE*::[(P*immR-immR*Ω141) *spc*] *thrC*::[(P*spank-int*) *erm*] *comK*::*cat str*
JMA875	*comK*::*cat str*
JMA878	ICE*Bs1*^{0} *thrC*::[(P*spank-int*) *erm*] *comK*::*cat str*
JMA882	Δ*int205*::*cat*::*tet thrC*::[(P*spank-int*) *erm*] *comK*::*cat str*
KLG125	*amyE*::[(P*spank*(*hy*)) *spc*] *thrC*::[(P*xis–lacZ*Ω343) *erm*]
KLG126	*amyE*::[(P*spank*(*hy*)-*rapI*) *spc*] *thrC*::[(P*xis–lacZ*Ω343) *erm*]

[a] All *B. subtilis* strains are derived from JH642 and contain *trpC2* and *pheA1* (Perego *et al*., 1988).